

Research Article

Deep Learning Network for Multiuser Detection in Satellite Mobile Communication System

Guan Qing yang ^{1,2}, Wu Shuang,¹ and He Ya-Ru¹

¹College of Engineering, Xi'an International University, Xi'an 710077, China

²College of Electronic and Information Engineering, Shenyang Aerospace University, Shenyang 110136, China

Correspondence should be addressed to Guan Qing yang; guan_qy@163.com

Received 16 November 2018; Accepted 24 December 2018; Published 4 March 2019

Guest Editor: Zoran Peric

Copyright © 2019 Guan Qing yang et al. This is an open access article distributed under the Creative Commons Attribution License, which permits unrestricted use, distribution, and reproduction in any medium, provided the original work is properly cited.

A multiuser detection (MUD) algorithm based on deep learning network is proposed for the satellite mobile communication system. Due to relative motion between the satellite and users, multiple access interference (MUI) introduced by multipath fading channel reduces system performance. The proposed MUD algorithm based on deep learning network firstly establishes the CINR optimal loss function according to the multiuser access mode and then obtains the best multiuser detection weight through the steepest gradient iteration. Multilayer nonlinear learning obtains interference cancellation sharing weights to achieve maximum signal-to-noise ratio through gradient iteration, which is superior than the traditional serial interference cancellation algorithm and parallel interference cancellation algorithm. Then, the weights with multiuser detection through multilayer network forward learning iteration are obtained with traditional multiuser detecting quality characteristics. The proposed multiuser access detection based on deep learning network algorithm improves the MUD accuracy and reduces the number of traditional multiusers. The performance of the satellite multifading uplink system shows that the proposed deep learning network can provide high precision and better iteration times.

1. Introduction

Due to high-speed relative motion between mobile users and satellites in the satellite mobile communication system, different users access with the satellite at different elevation angles and multipath channel between satellite and user links is fading. These factors are creating obstacles for multiuser detection. In the case of limited bandwidth system, multiuser access detection (MUD) is an important issue in satellite mobile communication systems.

In the early literature, Cao and Viswanathan [1] proposed a method based on transformation of training sequences for single-user detection; the performance based on transforming training sequences is poor because the algorithm needs to add redundant information to make the signal transmission efficient. In the literature [2, 3], a soft iterative method was proposed for multiuser signal detection, but soft iteration required too much user information and it was not easy to achieve convergence.

Since multiusers accessed the satellite system at different elevation angles, different access carrier frequency offsets (CFOs) introduced multiuser access interference (MUI), so it was difficult to implement single-tap FDE to achieve multiuser detection. Some related research studies had been designed for multiuser detection. Tang and Heath [4] proposed a joint MUD scheme for MIMO. On this basis, in [5], CP was used to perform multiuser detection by accurately estimating the frequency offset. Zhang and Gao [6] proposed a blind scheme for multiuser uplink with large antennas. However, literatures [4–6] were proposed based on CP, and their solutions relied on searching for sampling. In this case, it suffered significant performance degradation, especially in the case of relatively large delay spread.

Blind user detection did not require a priori information, which effectively improves transmission efficiency. Therefore, Zhang and Gao [6] proposed a blind detection algorithm. At present, based on this, in [7, 8], a combination of advanced technologies, such as space-time processing and

interference cancellation, which improved transmission performance of the system, is proposed. Karakaya et al. [9] proposed an improved Kalman filter (KF) for multiuser detection, which requires a longer training sequence. Cao et al. [10] proposed LS-based algorithm (least squares) and MMSE (least mean square error) for multiuser interference, but they are not accurate. Chang et al. [11] proposed a multiuser detecting method, which needs cancel interference caused by carrier frequency with a high degree of complexity. A new algorithm based on time domain carrier frequency offset compensation algorithm was proposed in [9] for multiuser detection, but its accuracy was low. Cui in [10] proposed the joint iterative detection algorithm, which required a lot of matrix transposition operations and high complexity.

In recent years, literatures researched on the compressed sensing reconstruction algorithm for multiuser detection. Abebe and Kang [12] proposed an iterative sorting least squares (IORLS) algorithm for detecting multiuser signals. Based on this, orthogonal signal tracking (OMP) was used in [13] to reconstruct the signal for fast multiuser signal detection. An iterative support detection (ISD) algorithm had been proposed in [14], and a structured iterative detection (SISD) algorithm was proposed in [15] to recover multiple sparse signals. In [16], an approximate message delivery mechanism was proposed to reconstruct the signal. On this basis, Wei et al. [17] had proposed the application of this message for multiuser detection. On this basis, Donoho et al. [18] introduced expectation-maximization (EM) into multiuser detection and was named “joint-EM-AMP algorithm.” This algorithm could achieve good bit error rate (BER) performance by jointly utilizing structured sparsity of prior information. Wang et al. [19] proposed a dynamic compression-aware algorithm for more practical scenarios.

For nonlinear transformation of single-layer network, the related literature also discussed and optimized in detail. For blind channel estimation of MIMO communication systems, AsadUllah et al. [20] proposed fuzzy logic-empowered opposite learning algorithm, which adopted mutant particle swarm optimization to obtain MMSE and BER performance. However, the single-layer nonlinear transformation of the algorithm reduces system performance.

Especially for the NOMA system, in literature [12, 21–23], a multiuser detection (MUD) algorithm was proposed. Since UEs of the NOMA system randomly transmitted data, they must perform blind activity detection. Wang and Yin [14] proposed compressed sensing (CS) algorithms. Wang et al. [24] proposed a modified version of the original ISD algorithm. Wang et al. [24] summarized multiuser detection method for the satellite mobile communication system. Literature [25] presents a joint ML-based CFO estimation method, but the complexity of this method was relatively high and was not suitable for satellite systems. In [26–28], the PIC algorithm for multiuser detection was proposed. Durand et al. [29] proposed the SIC algorithm based on weighting to detect multiuser in LTE-A systems, which is to improve the signal-to-interference ratio SINR. Kiayani et al. [30] proposed an improved PIC algorithm; the complexity was large since interference matrix

transposition operation was very large, and the number of subcarriers was proportional.

For multilayer networks analysis, the related literature also discussed about CNN architecture. Yinghao et al. [31] proposed a multilayer neural network based on CNN for target recognition analysis, in order to deal with waste classification and obtain better resolution. Simulation results showed that the classification accuracy is higher than 90% under two different testing scenarios. Similarly, Albawi et al. [32] proposed a method for touch recognition, which was also implemented by CNN network. The proposed system outperformed other classification algorithms in terms of classification ratio. Simultaneously, the same CNN in [33] was also used in the Biomimetic Pattern Recognition to obtain a higher recognition rate. However, the above literatures all used the CNN network for visual feature recognition.

For the feature extraction of multilayer neural networks, Chao et al. [34] adopted a multilayer deep neural network with DBN architecture to acquire emotions through EEG signal acquisition. Compared with the CNN architecture, the DBN architecture was more suitable for processing transform domain features and achieving higher analysis accuracy. However, the algorithm was currently only for EEG signal analysis. Similarly, for multilayer neural network fusion decision, Wei et al. [35] proposed a weight-based fuzzy decision algorithm to achieve emotion recognition. The analysis was performed by multisource data decision fusion, which was including electroencephalography (EEG), electrocardiogram (ECG), respiration amplitude (RA), and galvanic skin response (GSR). However, the algorithm was used for data fusion direction.

2. System Model and Problem Formulation

2.1. Satellite-to-Ground Channel Model. If the shadow fading follows the Nakagami distribution, the Abdi star fading model was formed [36]. So, it is common for satellite-to-ground link model to use probability density functions, such as Rician model, Loo model, and Rician-Lognormal model. As a supplement to satellite-to-ground communication system, the satellite service scenario is mainly about wilderness area and open ground area, the shadow is less, and Clarke [37] also proved the correctness of this condition.

Some related literatures also have carried out studies on the satellite ground link channel model fitting through the measured data. Loo et al. [38], in view of the shadow effect on the signal propagation induced by trees, established the shadow effect model, but the application of the model has some limitations. Abdi et al. [39] established the urban road shadow (ERS) model for the satellite ground link with carrier frequency field between 870 MHz and 1500 MHz, and the model is suitable for the 1.5 GHz band channel fading distribution. In the literature [40], an integrated (CEFM) model is obtained by the integrated ERS model and the EFM model, which can be applied to a larger elevation range of 20 degrees to 80 degrees. Hess has used ATS-6 satellite to establish a small-scale and large-scale satellite ground link channel model within the city of 1200 km [41]. According to

the ESA satellite ground link access elevation data, ERS model is put forward in literature [42], and the transmission channel model of terrestrial mobile satellites is given in [43], the establishment of L -band elevation model of this band access for multiple users.

In this paper, the satellite-to-ground channel model is established using the measured results of the German Aerospace Research Center [42], and the multiuser access elevation model is established using the test data of the ESA (European Space Agency) in [37]. In this paper, the theory of tapped delay line channel model is used to establish the satellite-to-ground channel model. Figure 1 shows frequency selective channel for satellite-to-ground link model based on tapped delay line.

The specific method is to simulate the signal amplitude fading through the tapped delay line filter. Firstly, it is assumed that the scattering body is divided into several clusters, and the bandwidth of the signal transmission bandwidth is not resolved within each cluster. Then, the multicluster is used to model the satellite-to-ground link.

In the tapped delay line model, each tap represents a set of a plurality of delay paths with the same sum, but also the time delay path changes due to different flat fading amplitudes.

The tapped delay line model for satellite-to-ground link, multipath channel impulse response is composed of different delay characteristics; the channel modeling method is established for satellite-to-ground channel model following the tapped delay line.

Define $h(t, \tau)$ multipath propagation delay and time channel impulse response function, for different τ 's; $h(t, \tau)$ is not related to each other. For determining the time delay τ , $h(t, \tau)$ is a stochastic process with mean complex Gauss time variation, and the impulse response $h(t)$ is with the amplitude characteristics of flat fading. Therefore, the time-varying impulse of the multipath channel can be expressed as follows:

$$h(t, \tau) = \sum_{l=0}^{L-1} b_l v_l(t) \delta(\tau - \tau_l), \quad (1)$$

where τ_l is the path of the transmission delay; $v_l(t)$ is a complex Gauss process; l is expressed as the path delay component, and the fading of the path is induced by the Doppler power and power spectrum; b_l is expressed as the delay coefficient, the square root of the value for the average l th path delay power.

$v_l(t)$ can be expressed in a delay interval at different incident angles' weighted path. The measured results with the German Aerospace Research Center are proposed in [36], which are about the rural environment, urban environment, suburban environment, with a signal carrier frequency of 1.82 GHz.

2.2. Multiuser Access Model. The Doppler shift caused by satellite motion is regular. At the same time, for defined mobile user, the Doppler shift is determined by the velocity of the high-speed motion and the elevation angle of the user.

The Doppler shift introduced by high-speed satellite motion can be approximately equal.

Defining $x(n)$ as the transmitted signal, ξ as the frequency offset factor, and $h(n, l)$ as the impact response channel, the received $y(n)$ can be expressed as

$$y(n) = \sum_{l=0}^{L-1} x(n)h(n, l). \quad (2)$$

After introducing frequency offset interference, the received signal can be expressed as

$$y(n) = \sum_{l=0}^{L-1} x(n)h(n, l) \exp\left(\frac{j2\pi n \xi}{N}\right). \quad (3)$$

The receiving end performs N -point DFT demodulation on the received band offset signal, and after serial conversion, we could obtain frequency domain signal, which can be expressed as

$$Y(k) = X(k)H(k)C(0) + \sum_{\substack{l=0 \\ l \neq k}}^{N-1} X(l)H(l)C(l-k), \quad (4)$$

where $H(k)$ is the channel frequency response and $C(k)$ is the interference introduced in the frequency domain. The first term indicates the part without carrier interference. The frequency offset causes change for amplitude and the rotation caused by carrier k . The second term is the intercarrier interference caused by the remaining subcarriers of carrier k . As can be seen from the above formula, when $\xi = 0$, $C(0) = 1$. This means, when the carrier frequency offset is zero, the interference term coefficient is 1, which means no interference would occur. This also shows that the interference between carriers depends on the relative frequency deviation and the serial number distance between subcarriers as the relative frequency offset interference factor increases.

When the carrier frequency offset is zero, the interference coefficient is 1. This shows that the interference between carriers depends on the relative frequency deviation and the serial number distance between subcarriers. As the relative frequency offset interference factor increases, $C(0)$ reduced interference to the received signal, but $C(l-k)$ increased interference to the received signal; intercarrier interference plays a major role where

$$C(l-k) = \frac{\sin(\pi(l+\xi-k))}{N \sin((\pi/N)(l+\xi-k))} \cdot \exp\left(j\pi\left(\frac{N-1}{N}\right)(l+\xi-k)\right). \quad (5)$$

Equation (5) also shows the energy leakage of subcarrier k to subcarrier l due to the frequency offset effect. The magnitude of the energy interference depends on the sequence difference of the carrier spacing and the relative carrier frequency offset factor. If the relative carrier frequency offset factor is e , then the relative energy leakage of the k th carrier to the l st carrier can be expressed as

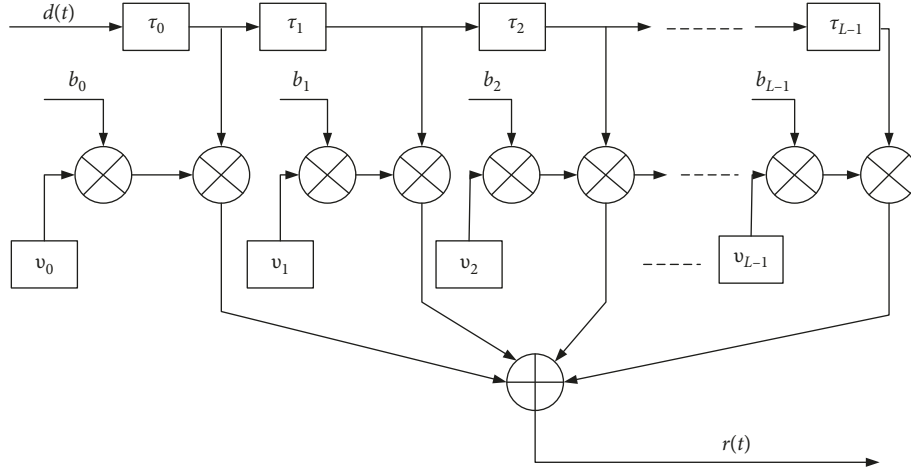


FIGURE 1: Channel model for satellite-to-ground link based on tapped delay line.

$$|C_{k,l}|^2 = \frac{\sin^2(\pi[(l-k) + \xi])}{N^2 \cdot \sin^2(\pi[(l-k) + \xi]/N)}. \quad (6)$$

If the interference signal with frequency offset is DFT transformed, it can be written as follows:

$$Y(k) = X(k) \cdot C, \quad (7)$$

where C is the carrier frequency offset interference matrix, which can be expressed as

$$C = \begin{bmatrix} c(0) & \cdots & c(N-1) \\ c(N-1) & \ddots & c(N-2) \\ \vdots & c(0) & \vdots \\ c(1) & \cdots & c(0) \end{bmatrix}. \quad (8)$$

Equation (8) can obtain some characteristics of the interference matrix C . The interference matrix introduced by the frequency offset is a Toeplitz-type matrix, in which each element of the matrix satisfies the periodic cycle property which can be expressed as

$$c(k) = c(k + N), \quad (9)$$

where $(\cdot)^{-1}$ is the inverse matrix and $(\cdot)^T$ is the transposed matrix conjugate, which can be expressed as

$$C^{-1} = C^*. \quad (10)$$

Defining $\Phi = \exp(j2\pi\Delta fT)$, the elements of the matrix can be written in recursive form:

$$c(k) = \Phi \cdot c(k-1) = \Phi^2 \cdot c(k-2) = \cdots = \Phi^i \cdot c(0). \quad (11)$$

Through the elemental analysis of the matrix, in the case of smaller frequency offset interference, the energy is mainly concentrated on the diagonal. The larger the frequency offset value, the more dispersed the energy, the larger the interference term, and the more the interference of the introduced ICI. Its energy distribution diagram is shown in Figures 2 and 3.

We could obtain from equation (11) that $\exp(j2\pi\xi m'/M)$ is the linear transformation of the introduced phase.

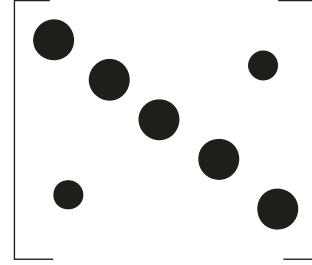


FIGURE 2: Matrix energy distribution introduced by small frequency offset.

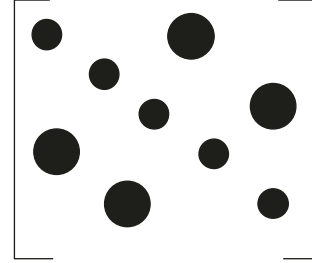


FIGURE 3: Matrix energy distribution introduced by large frequency offset.

The number of set carriers is defined as 512, the channel bandwidth is 20 MHz, the Doppler shift is 15 kHz, and the signal mapping mode is QPSK. Figure 4 shows that the demodulated signal phase changes linearly with the increasing of subcarrier number.

For the multiuser uplink access, the interference comes from frequency offsets. At the same time, the larger the frequency offset range for each user, the more serious the multiuser interference. For the satellite transmission system uplink system, the access interference cancellation of each user is the key for uplink user detection.

3. Proposed MUD Algorithm Based on Deep Learning Network

The process of multiuser detection is divided into three parts. First, the multiuser signal is completed to cancel the

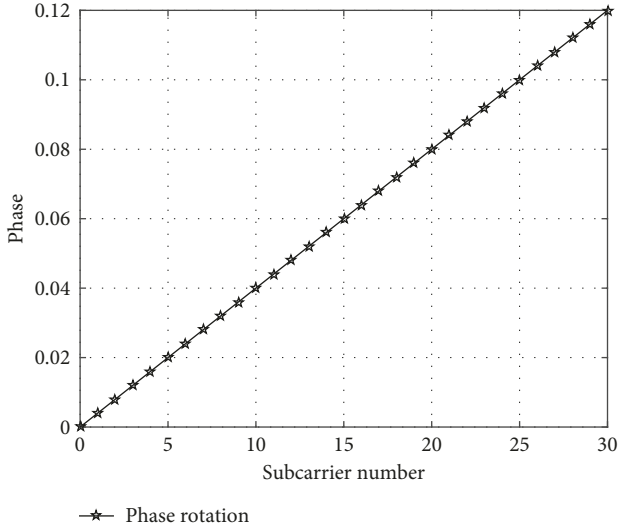


FIGURE 4: Linear phase introduced by frequency offset.

access interference and the multiuser access interference is reduced by establishing the optimal weight of the multilayer network. Secondly, through the multilayer network, the weight is iterated to obtain the optimal point. Through the network weight sharing and iteration of the first two parts, the optimal identification weight is finally obtained. Multiuser detection and identification is accomplished by optimally identifying the weight network.

3.1. Proposed Shared IC Algorithm. The proposed algorithm is based on the goal for optimizing CINR, which is to find the optimal CINR corresponding to WIC interference cancellation algorithm weights. Thus, multiuser interference signal received by satellite can be expressed as

$$Y^i = D^i H^i C_{i,i} + D^i H^i C_{i,k} + D^j H^j C_{i,j} + N, \quad (12)$$

$$k, i = 0, 1, \dots, N-1, \quad j = 0, 1, \dots, M-1,$$

where $D_1^{(i)} = [y_1^{(i)}, y_1^{(i)}, \dots, y_M^{(i)}] \in \mathbb{C}^{N \times M}$ and $H^{(i)} = [h_1^{(i)}, h_1^{(i)}, \dots, h_M^{(i)}]$. Here, M is the number of subcarrier cancellations and w is the weight. $C_{k,l}$ is defined as the interference induced between subcarrier i of user j and carrier k of user i , which can be expressed as

$$C_{j,k} = \sum_{j=1}^{N-1} \sum_{j \neq k}^{N-1} \frac{\sin \pi(j-k' + \xi^j)}{N \sin(\pi/N)(j-k' + \xi^j)} \frac{\exp(j\pi(j-k' + \xi^j))(N-1)}{N}. \quad (13)$$

According to multicarrier allocation, this process can be a multiuser signal separation. Firstly, each user can be according to the traditional WIC algorithm for cancellation. For user i , subcarrier k , with the WIC algorithm, it can be expressed as

$$Y_m^i(k) = Y_{(m-1)}^i(k) - w \Lambda_{k,l} Y_{m-1}^i(l) - w \Lambda_{k,l} Y_{m-1}^j(l), \quad (14)$$

where $w C_{k,l} Y_{m-1}^j(l)$ is considered as the previous interference term from subcarrier l .

$Y_m^i(k)$ is defined as the m th interference cancellation signals for user i and subcarrier k , and $Y_{(m-1)}^i(k)$ is the $(m-1)$ th r interference cancellation signals for user j . Getting formula (14) into the WSIC judgment, it could be obtained as the m th interference cancellation signals:

$$Y_2^i = D^i(k) H(k) (1 - w C_{k,l}^2) + \sum_{\substack{l=0 \\ l \neq k}}^{N-1} \sum_{l \in j} D^i(l) H^i(l) (C_{k,l} (1 - w) - w C_{k,l}^2). \quad (15)$$

Idealizing it, we could obtain

$$\text{CINR}^i \propto (1 - w C_{k,l}^2)^2. \quad (16)$$

Secondly, according to the traditional WPIC algorithm, each user can be for parallel cancellation interference, and it can be expressed as

$$Y_m^i = Y_{(m-1)}^i - w C_{i,l} Y_{m-1}^j, \quad (17)$$

where m is the iteration for WPIC interference cancellation and w is defined as the weight, $\Theta_{k,l}$ is considered as the interference, and $w C_{i,l} Y_{m-1}^j$ is considered as the previous interference term.

Y_m^i is the m th interference cancellation signals for user i and $Y_{(m-1)}^i$ is the $(m-1)$ th interference cancellation signals for user j . Getting formula (13) into the WSIC judgment, it could be obtained as the m th interference cancellation signals:

$$Y_2^i = D^i(k) H^i(k) (1 - w C_{k,l}^2) + I, \quad (18)$$

where I is the second interference judgments and Y_2^i is the received signal after cancellation, which can be obtained as

$$I = \sum_{\substack{l=0 \\ l \neq k}}^{N-1} \sum_{l \in j} D^i(l) H^i(l) (C_{k,l} (1 - w) - w C_{k,l}^2). \quad (19)$$

Due to different user access elevation angles, as well as the satellite ground link fading channel, introducing different serious Doppler frequency shifts is for the satellite-to-ground uplink system. For a particular user, because the tangential velocity of the satellite in a symbol is the same, the relative carrier frequency is kept constant, so the frequency offset introduced in a symbol period can be regarded as constant. Therefore, the normalized frequency offset factor can be considered to be constant.

The definition of satellite ground link uplink carrier number is 1024; the satellite suburban environment model is given in Table 1. Figure 5 shows that as the number of carrier interval sequence is reduced, energy leakage is more serious.

It can be obtained from formula (13) that a function of the value of the interference and the W weight value with IC algorithm, which can be expressed as a convex function. Signal-to-noise ratio can be obtained to the best value, when

the W weight is to the pole value. The proposed IC algorithm is based on the optimal weights, which can greatly reduce the number of iterations and improve the accuracy of the algorithm. The signal-to-interference ratio can be used by the comb or block pilot signal. By training the initial weights in the iteration, the optimal interference ratio can be obtained, which is close to the optimum.

The number of users is 4, and the number of subcarriers is 2048. In the condition of AWGN, SNR = 5 dB, the allocation is OFDM, and the frequency offset is 0.01, 0.05, 0.15, and 0.2. The multifading channel is shown in Table 1. The curve of the relationship between average CINR and weight w is shown in Figure 6.

The proposed multiuser detection algorithm is to optimize SINR through obtaining optimal cancellation weight; therefore, the IC algorithm can be divided into WSIC and WPIC algorithms; the WSIC algorithm is cancel interference for multiuser access according to each subcarrier, and the WPIC is the multiuser interference cancellation algorithm at the same time.

Figure 6 states that the convex function can reach the optimal value with w weight. Define CINR_{opt} as the optimal after WIC algorithm cancellation. Since CINR_{opt} is the convex function with w , the optimal CINR could be obtained when w has the extreme. Define the initial value as $w = 1$. In this case, the algorithm becomes the traditional SIC or PIC algorithm weight.

The improved algorithm is based on the WIC algorithm. Optimal weights are iterated to approximate initial weights. It is specific for obtaining the optimal weights below.

Defining E_{CINR} as the error between CINR_{opt} and CINR_{out} , which after cancellation with the WIC algorithm can be expressed as

$$E_{\text{CINR}} = \text{CINR}_{\text{out}} - \text{CINR}_{\text{opt}}, \quad (20)$$

CINR_{opt} could be obtained with the Taylor expansion:

$$\text{CINR}_{\text{out}} \approx w_{\text{opt}} + \alpha(w_{\text{out}} - w_{\text{opt}}), \quad (21)$$

where

$$\alpha \approx \left[\frac{\partial \text{CINR}_{\text{out}}}{\partial w_{\text{out}1}}, \frac{\partial \text{CINR}_{\text{out}}}{\partial w_{\text{out}2}}, \dots, \frac{\partial \text{CINR}_{\text{out}}}{\partial w_{\text{out}k}} \right]. \quad (22)$$

The influence of the satellite to ground link on this algorithm consists of two parts. Firstly, the influence for the proposed algorithm is also induced by the multiuser access angle differences. Due to differences in relative motion between the user and satellite, multiuser access interference has been generated, which significantly degrades the satellite system performance.

When multiusers access the same satellites, the multiuser access angle differences will introduce different carrier frequency offsets in the total number of the carrier system. Under certain conditions, the carrier frequency deviation will induce the different multiple access interference, including interference simulation as shown in Figure 6; the number of users is increasing, and the serious interference induced by frequency offset is larger.

Secondly, the influence for the proposed algorithm is induced by multipath fading. For urban simulation scenarios, the signal reflection effect caused by buildings is larger, and the diffraction effect caused by multipath is also larger. The more delay the received signal propagation, the more serious the signal fading is.

In the countryside scene, compared with the urban scene, the multipath number is decreased and the fading is relatively flat. This is because that the countryside scene is with a smaller number of building and weaker reflection and refraction.

3.2. Shared Weight Process and Feedback Solution Process.

For multiuser received signals to cancel interference, we use shared weights to obtain the best weights and then obtain user detection and weight update.

The cost function established can be expressed as

$$\min_x \lambda_t \|w_t\|_1 + \|y_t - w_t x\|_2^2, \quad (23)$$

The cost function is to find that the accurate reconstruction, which should be realized. Then, the optimal weight detection error is made. Therefore, the sparse recovery for multiweight sharing can be obtained, and the optimal user detection for all the users can be satisfied in the following:

$$\min_x \lambda_t \|w_t\|_{1,w} + \|y_t - w_t x\|_2^2, \quad (24)$$

where

$$\|w\|_{1,w} = \sum_{i=1}^K w_i |x_i|. \quad (25)$$

The first term is a nonzero regular term whose position is known and is different from the traditional mode of all cost functions.

In addition to the weight constraint cost, the regularization constraint can be established for the corresponding x .

Therefore, when the measurement data are very small, x would become larger. For solving the problem, we used the improved solutions to solve the regularization. The modified cost function is expressed as

$$\min_x \lambda_t \|w\|_{1,w} + \alpha_t \|x - \hat{x}_t\|_2^2 + \|y_t - w_t x\|_2^2. \quad (26)$$

The augmented Lagrangian is expressed as

$$L(x, z, t_t) = \alpha_t \|x - \hat{x}_t\|_2^2 + \|y_t - w_t x\|_2^2 + t_t \|w - \hat{w}_t\|_2^2. \quad (27)$$

The scaled problem (6) consists of three iterations:

Shared weight updates: x , w , and u .

$$\begin{aligned} x_t^{[k+1]} &= \underset{x}{\text{argmin}} \left(\alpha_t \|x - \hat{x}_t\|_2^2 + \|y_t - w_t x\|_2^2 + \beta \|w - w_t^{[k]} + u_t^{[k]}\|_2^2 \right), \\ w_t^{[k+1]} &= \underset{w}{\text{argmin}} \left(\|w - \hat{w}_t\|_2^2 + \beta \|w_t^{[k+1]} - w_t^{[k]} + u_t^{[k]}\|_2^2 \right), \\ u_t^{[k+1]} &= u_t^{[k+1]} + x_t^{[k+1]} - w_t^{[k+1]}. \end{aligned} \quad (28)$$

TABLE 1: Suburban environment parameter.

Tap	Distribution function	Parameter	Parameter distribution	Numerical value (dB)	Time delay (ns)
1	LOS: Rician	Rice factor	K	9.7	0
2	Rayleigh	Average multipath power	$2\sigma_l^2$	-23.6	100

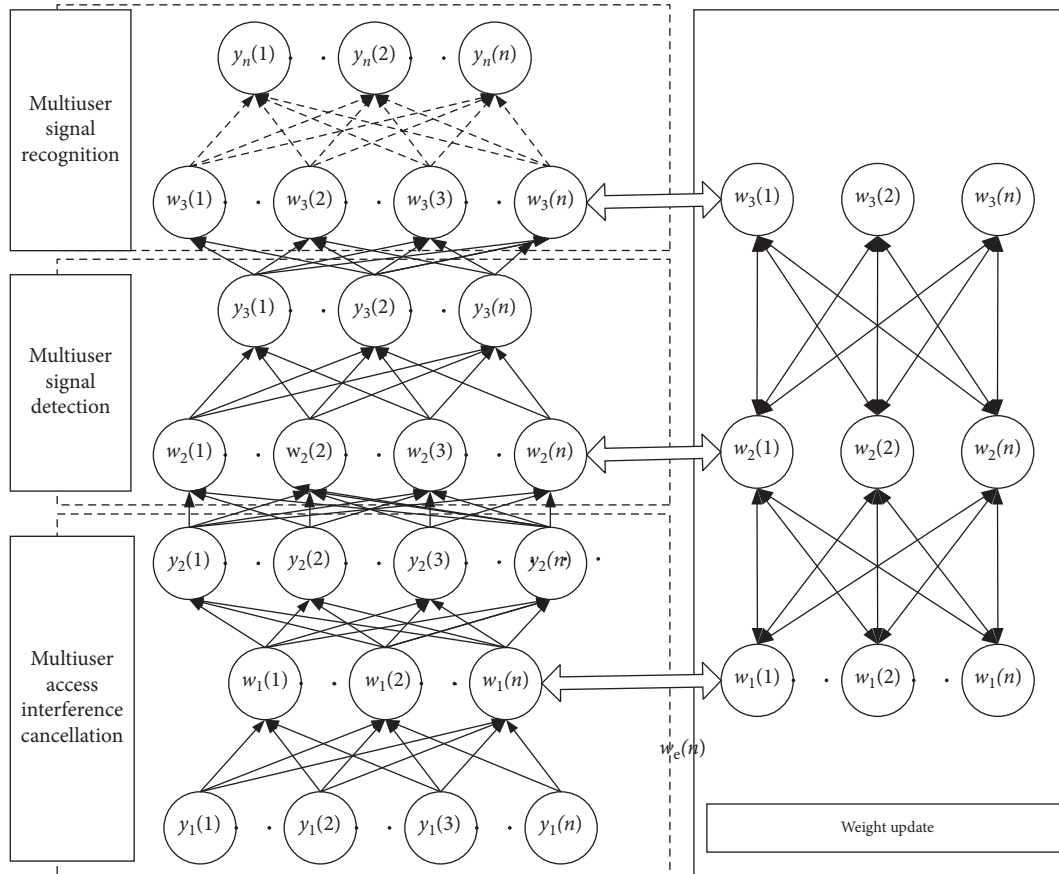


FIGURE 5: Multiuser detection system block diagram.

4. Experimental Classification Results and Analysis

Establishing that the orbital altitude is 1100 km, the rural environment measured data proposed in [36] are satellite-to-ground uplink system model as in Table 2 in this paper.

Set the satellite beam spot beam of number 5 with a coverage diameter of 450 km. Satellite-to-ground link model with L -band carrier frequency in rural environments is shown in Table 2. Set the number of uplink users 4 and transmit pilot block type information. For analysis, the user has access to a maximum height at 35° , 25° , 5° , and 15° . The signal bandwidth is 50 MHz, the number of subcarriers is 1024, and the signal mapping method is defined as QPSK, BPSK, 16QAM, OFDM signal.

Figure 7 shows the BER simulation results for multiuser detection based on the WIC algorithm. Compared with the iterative sorting least squares (IORLS) algorithm proposed in [12] and the orthogonal signal tracking (OMP) algorithm proposed in [13], the WIC algorithm is improved by two iterations for sharing weight. The simulation results can be

obtained from Figure 7. In first iteration, the multiuser detection algorithm performs better than the WPIC algorithm. Through the optimization iteration, the weight converges to the bump function close to the inflection point, and we can obtain the optimal multiuser detection and thus obtain the best BER performance for multiuser detection. Since the proposed MUD algorithm is superior to the improved conventional algorithm, interference cancellation improves the complexity. The system is enhanced under the condition of $10e-3$ BER.

Figure 8 shows the CINR performance comparison between the MUD algorithm proposed in [12] and the proposed MUD algorithm, since the improved MUD algorithm cancels subcarrier frequency offset interference and CINR system can be optimal.

Figure 9 shows different BER curves for each uplink user at $\text{SNR} = 5$ dB. As the relative interference carrier frequency offset increases, the BER of user error rate increases, which is due to the multiuser access system. And its performance of the algorithm is similar to the traditional algorithm, which is due to interference introduced by carrier frequency offset. After

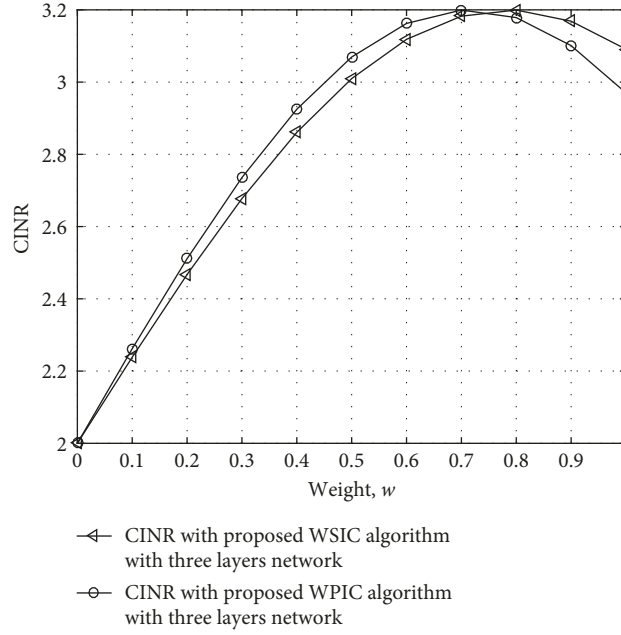


FIGURE 6: CINR performance at different weights in the IC algorithm (including WSIC and WPIC) with three-layer network in two iterations.

TABLE 2: Channel model parameter in rural environment.

Tap	Distribution function	Parameter	Parameter distribution	Numerical value (dB)	Time delay (ns)
1	LOS: Rician	Rice factor	K	6.3	0
	nLOS: Rayleigh	Average multipath power	$2\sigma_1^2$	-9.5	
2	Rayleigh	Average multipath power	$2\sigma_1^2$	-24.1	100
3	Rayleigh	Average multipath power	$2\sigma_1^2$	-25.2	250

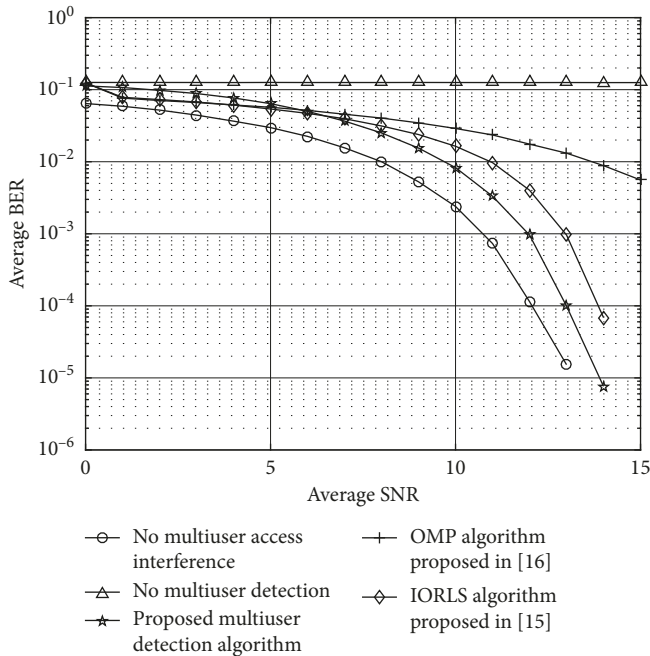


FIGURE 7: BER curves under different SNRs.

multilayer iteration, the weight is close to the optimal value at this time, and then the system is close to the maximum SINR optimization, which can be obtained as an optimization.

Figure 10 is the probability of correct classification of proposed deep learning network at different SNRs, which is also based on different length curves for each user. As the relative interference carrier frequency offset increases, the PCC of user error rate increases, which is due to the user access to the multiuser access system. The performance of the improved traditional multiuser detection algorithm at large frequency offset is poor, which is due to residual carrier frequency offset. When training length is larger, the system is close to the maximum SINR optimization, which can be obtained as an optimization.

5. Conclusion

A multiuser detection algorithm based on deep learning network has been proposed. The proposed deep learning network for MUD could provide high precision and lower iteration times, which firstly establishes the CINR optimal loss function according to the multiuser access interference mode and then obtains the best multiuser detection weight through the steepest gradient iteration. The important feature of the proposed algorithm is through nonlinear optimal direction learning and to achieve maximum signal-to-noise ratio through gradient iteration, and then share weights. Through establishing a typical satellite communication system simulation platform, compared with the OMP and IORLS algorithms, the proposed deep learning network algorithm has

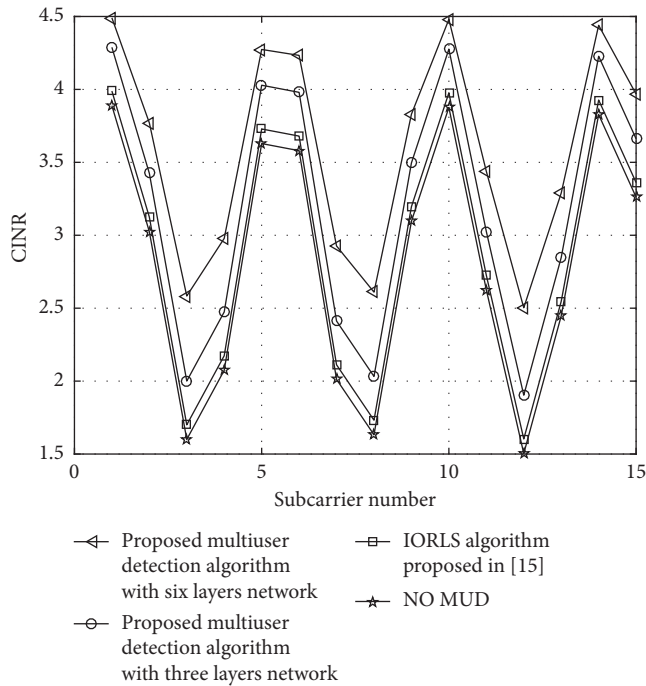


FIGURE 8: CINR performance of different subcarriers.

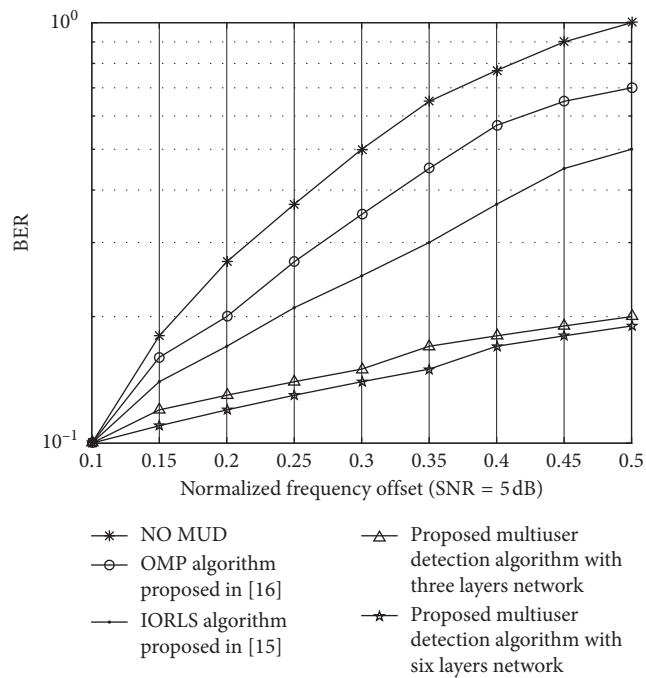


FIGURE 9: BER performance of different normalized frequency offsets.

better performance in different conditions of SNR, CINR, and carrier frequency offset interference.

Data Availability

The data used to support the findings of this study are available from the corresponding author upon request.

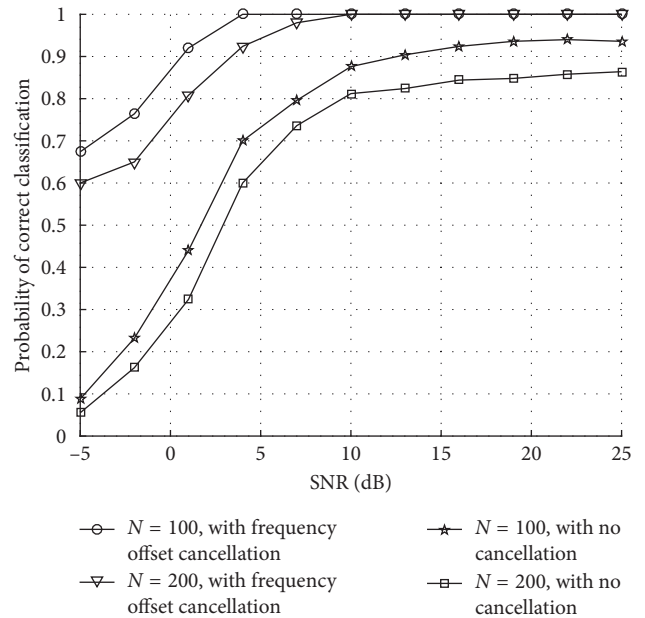


FIGURE 10: Probability of correct classification of the proposed deep learning network for multiuser access to satellite at different length curves.

Conflicts of Interest

The authors declare that they have no conflicts of interest.

Acknowledgments

This work was supported by the National Natural Science Foundation of China (no. 61501306), the Natural Science Foundation of Liaoning Province of China (no. 2015020026), and the Natural Science Foundation of Liaoning Provincial Department of Education (no. L2015402).

References

- [1] L. Cao and R. Viswanathan, "Divergence-based soft decision for error resilient decentralized signal detection," *IEEE Transactions on Signal Processing*, vol. 62, no. 19, pp. 5095–5106, 2014.
- [2] A. Gomaa, L. M.-A. Jalloul, and A. Jalloul, "Efficient soft-input soft-output MIMO chase detectors for arbitrary number of streams," *IEEE Signal Processing Letters*, vol. 22, no. 8, pp. 1084–1088, 2015.
- [3] S. Park, B. Shim, and J. W. Choi, "Iterative channel estimation using virtual pilot signals for MIMO-OFDM systems," *IEEE Transactions on Signal Processing*, vol. 63, no. 12, pp. 3032–3045, 2015.
- [4] T. Tang and R. W. Heath, "A space-time receiver with joint synchronization and interference cancellation in asynchronous MIMO-OFDM systems," *IEEE Transactions on Vehicular Technology*, vol. 57, no. 5, pp. 2991–3005, 2008.
- [5] J. Chen, Y.-C. Wu, S. Ma, and T.-S. Ng, "Joint CFO and channel estimation for multiuser MIMO-OFDM systems with optimal training sequences," *IEEE Transactions on Signal Processing*, vol. 56, no. 8, pp. 4008–4019, 2008.
- [6] W. Zhang and F. Gao, "Blind frequency synchronization for multiuser OFDM uplink with large number of receive

- antennas," *IEEE Transactions on Signal Processing*, vol. 64, no. 9, pp. 2255–2268, 2016.
- [7] B. Tang and J. Tang, "Joint design of transmit waveforms and receive filters for MIMO radar space-time adaptive processing," *IEEE Transactions on Signal Processing*, vol. 64, no. 18, pp. 4707–4722, 2016.
- [8] T. Allen and N. Al-Dhahir, "Performance analysis of a secure STBC with coherent and differential detection," in *Proceedings of IEEE Conference on Wireless Communications and Networking Conference (WCNC)*, pp. 522–527, New Orleans, LA, USA, March 2015.
- [9] B. Karakaya, H. Arslan, and H. A. Curpan, "Channel estimation for LTE uplink in high doppler spread," in *Proceedings of IEEE International Conference on Wireless Communications and Networking Conference*, pp. 1126–1130, Dalian, China, 2008.
- [10] Z. R. Cao, U. Tureli, and Y. D. Yao, "Analysis of two receiver schemes for interleaved OFDMA uplink," in *Proceedings of IEEE International Conference on Signals, Systems and Computers*, pp. 1818–1821, Monterey, CA, USA, November 2002.
- [11] Y.-K. Chang, F.-B. Ueng, K.-H. Wu, and Y.-Y. Li, "Pipelined turbo multiuser detection and Kalman channel estimation for MU-MIMO SC-FDMA systems," in *Proceedings of 2015 IEEE 4th Global Conference on Consumer Electronics (GCCE)*, pp. 227–230, Osaka, Japan, October 2015.
- [12] A. T. Abebe and C. G. Kang, "Iterative order recursive least square estimation for exploiting frame-wise sparsity in compressive sensing-based MTC," *IEEE Communications Letters*, vol. 20, no. 5, pp. 1018–1021, 2016.
- [13] J. A. Tropp and A. C. Gilbert, "Signal recovery from random measurements via orthogonal matching pursuit," *IEEE Transactions on Information Theory*, vol. 53, no. 12, pp. 4655–4666, 2007.
- [14] Y. Wang and W. Yin, "Sparse signal reconstruction via iterative support detection," *SIAM Journal on Imaging Sciences*, vol. 3, no. 3, pp. 462–491, 2010.
- [15] B. C. Wang, L. L. Dai, T. Mir, and Z. C. Wang, "Joint user activity and data detection based on structured compressive sensing for NOMA," *IEEE Communication Letters*, vol. 20, no. 7, pp. 1473–1476, 2016.
- [16] D. L. Donoho, A. Maleki, and A. Montanari, "Message-passing algorithms for compressed sensing," *Proceedings of the National Academy of Sciences*, vol. 106, no. 45, pp. 18914–18919, 2009.
- [17] C. Wei, H. P. Liu, Z. C. Zhang, J. Dang, and L. Wu, "Approximate message passing-based joint user activity and data detection for NOMA," *IEEE Communication Letters*, vol. 21, no. 3, pp. 640–643, 2017.
- [18] D. L. Donoho, Y. Tsaig, I. Drori, and J.-L. Starck, "Sparse solution of underdetermined systems of linear equations by stagewise orthogonal matching pursuit," *IEEE Transactions on Information Theory*, vol. 58, no. 2, pp. 1094–1121, 2012.
- [19] B. Wang, L. Dai, Y. Zhang, T. Mir, and J. Li, "Dynamic compressive sensing-based multi-user detection for uplink grant-free NOMA," *IEEE Communications Letters*, vol. 20, no. 5, pp. 2320–2323, 2016.
- [20] M. AsadUllah, M. A. Khan, S. Abbas et al., "Blind channel and data estimation using fuzzy logic-empowered opposite learning-based mutant particle swarm optimization," *Computational Intelligence and Neuroscience*, vol. 2018, Article ID 6759526, 12 pages, 2018.
- [21] L. Dai, B. Wang, Y. Yuan et al., "Non-orthogonal multiple access for 5G: solutions, challenges, opportunities, and future research trends," *IEEE Communications Magazine*, vol. 53, no. 9, pp. 74–81, 2015.
- [22] A. Bayesteh, E. Yi, H. Nikopour, and H. Baligh, "Blind detection of SCMA for uplink grant-free multiple-access," in *Proceedings of ISWCS*, pp. 853–857, Barcelona, Spain, August 2014.
- [23] B. Shim and B. Song, "Multiuser detection via compressive sensing," *IEEE Communication Letters*, vol. 16, no. 7, pp. 972–974, 2012.
- [24] B. Wang, L. Dai, T. Mir, and Z. Wang, "Joint user activity and data detection based on structured compressive sensing for NOMA," *IEEE Communication Letters*, vol. 20, no. 7, pp. 1473–1476, 2016.
- [25] P. Muneer and S. M. Sameer, "Joint ML estimation of CFO and channel, and a low complexity turbo equalization technique for high mobility OFDMA uplinks," *IEEE Transactions on Wireless Communications*, vol. 14, no. 7, pp. 3642–3654, 2015.
- [26] F. Rui and L. Zhang, "Generalised grouped minimum mean-squared error-based multi-stage interference cancellation scheme for orthogonal frequency division multiple access uplink systems with carrier frequency offsets," *IET Communications*, vol. 7, no. 7, pp. 685–695, 2013.
- [27] T. N. Nguyen, X. Lai, B. Tran, and Q. K. Nguyen, "Performance analysis of the VBLAST algorithm for MIMO-OFDMA systems on spatial correlated channels," in *Proceedings of 2014 International Conference on Computing, Management and Telecommunications (ComManTel)*, pp. 146–151, 2014.
- [28] S. W. Hou and C. Ko, "Intercarrier interference suppression for OFDMA uplink in time and frequency selective Rayleigh fading channels," in *Proceedings of IEEE International Conference on Vehicular Technology*, pp. 1438–1442, Alberta, Canada, 2008.
- [29] C. Durand, F. Durnez, and P. Sehier, "Multiuser detection for a multimedia LEO satellite system," in *Proceedings of IEEE International Conference on Universal Personal Communications*, pp. 653–657, Florence, Italy, October 1998.
- [30] A. Kiayani, L. Anttila, Y. Zou, and M. Valkama, "Channel estimation and equalization in multiuser UplinkOFDMA and SC-FDMA systems under transmitter RF impairments," *IEEE Transactions on Vehicular Technology*, vol. 65, no. 1, pp. 82–99, 2016.
- [31] Y. Chu, C. Huang, X. Xie et al., "Multilayer hybrid deep-learning method for waste classification and recycling," *Computational Intelligence and Neuroscience*, vol. 2018, Article ID 5060857, 9 pages, 2018.
- [32] S. Albawi, O. Bayat, S. Al-Azawi et al., "Social touch gesture recognition using convolutional neural network," *Computational Intelligence and Neuroscience*, vol. 2018, Article ID 6973103, 10 pages, 2018.
- [33] L. Zhou, Q. Li, G. Huo, and Y. Zhou, "Image classification using Biomimetic pattern recognition with convolutional neural networks features," *Computational Intelligence and Neuroscience*, vol. 2017, Article ID 3792805, 12 pages, 2017.
- [34] H. Chao, H. Zhi, L. Dong, and Y. Liu, "Recognition of emotions using multichannel EEG data and DBN-GC-based ensemble deep learning framework," *Computational Intelligence and Neuroscience*, vol. 2018, Article ID 9750904, 11 pages, 2018.
- [35] W. Wei, Q. Jia, Y. Feng, and G. Chen, "Emotion recognition based on weighted fusion strategy of multichannel physiological signals," *Computational Intelligence and Neuroscience*, vol. 2018, Article ID 5296523, 9 pages, 2018.

- [36] J. F. Ossanna, "A model for mobile radio fading due to building reflections: theoretical and experimental fading waveform power spectra," *Bell System Technical Journal*, vol. 43, no. 6, pp. 2935–2971, 1964.
- [37] R. H. Clarke, "A statistical theory of mobile radio reception," *Bell System Technical Journal*, vol. 47, no. 2, pp. 957–1000, 1968.
- [38] C. Loo, "A statistical model for a land mobile satellite link," *IEEE Transactions on Vehicular Technology*, vol. 34, no. 3, pp. 122–127, 1985.
- [39] A. Abdi, W. C. Lau, M. S. Alouini et al., "A new simple model for land mobile satellite channels: first- and second-order statistics," *IEEE Transactions on Wireless Communications*, vol. 2, no. 3, pp. 519–528, 2003.
- [40] W. J. Vogel and J. Goldhirsh, "Fade measurements at L-band and UHF in mountainous terrain for land mobile satellite systems," *IEEE Transactions on Antennas and Propagation*, vol. 36, no. 1, pp. 104–113, 1988.
- [41] R. Barts, W. Stutzman, W. Smith et al., "Land mobile satellite propagation modeling," in *Proceedings of International Symposium on Antennas and Propagation Society*, pp. 20–23, Blacksburg, VA, USA, 1987.
- [42] J. Goldhirsh and W. J. Vogel, *Propagation Effects for Land Mobile Satellite Systems: Overview of Experimental and Modeling Results*, Vol. 1274, NASA Reference Publications, Washington, DC, USA, 1992.
- [43] T. Sofos and P. Constantinou, "Propagation model for vegetation effects in terrestrial and satellite mobile systems," *IEEE Transactions on Antennas and Propagation*, vol. 52, no. 7, pp. 1917–1920, 2004.



Hindawi

Submit your manuscripts at
www.hindawi.com

